

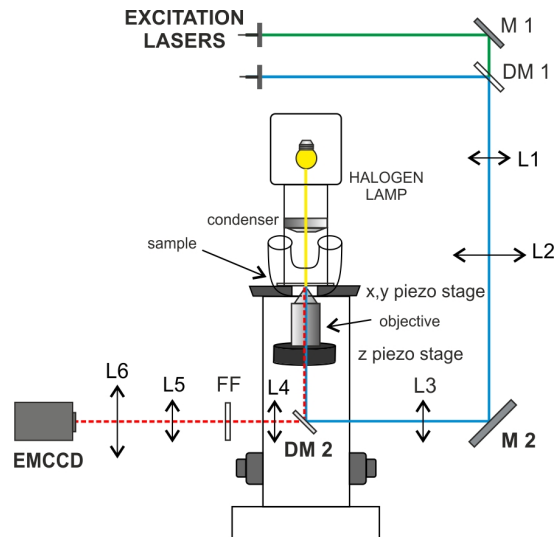
3D tracking of single nanoparticles and quantum dots in living cells by out-of-focus imaging with diffraction pattern recognition

*Lucia Gardini¹, Marco Capitanio^{*1,2}, and Francesco S. Pavone^{1,2,3,4}*

¹ LENS - European Laboratory for Non-linear Spectroscopy, Via Nello Carrara 1, 50019 Sesto Fiorentino, Italy; ² Department of Physics and Astronomy, University of Florence, Via Sansone 1, 50019 Sesto Fiorentino, Italy; ³ National Institute of Optics–National Research Council, Largo Fermi 6, 50125 Florence, Italy; ⁴ International Center of Computational Neurophotonics, Via Nello Carrara 1, 50019, Sesto Fiorentino (FI), Italy

Contact information: * capitan@lens.unifi.it

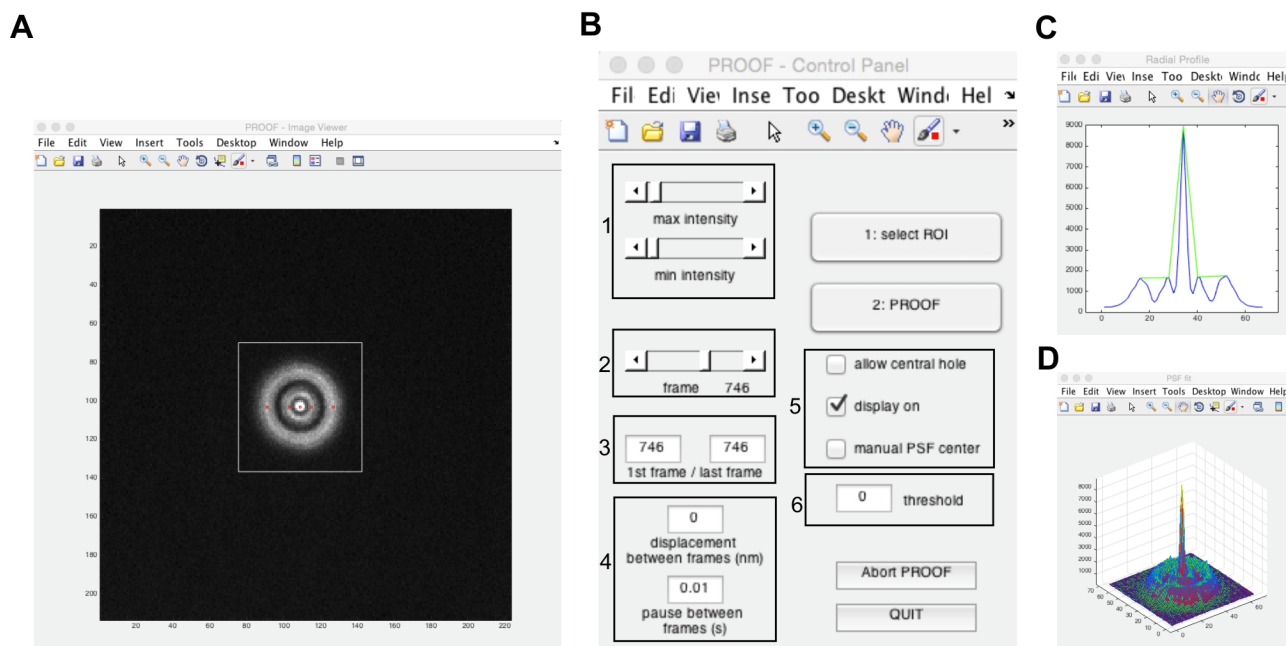
The experimental setup



Supplementary figure S 1 Scheme of the optical setup.

Our experimental setup, shown in figure S1, is equipped with 2 visible lasers for fluorescence excitation: Coherent Sapphire laser 532 nm (for fluorescent nanobeads excitation) and Argon 488 nm (for QDs excitation). The two lasers are coupled on the same path through a dichroic mirror (DM1). After the dichroic mirror, the beams are magnified by a telescope composed by achromatic doublets L1 and L2 and directed toward the objective axis through mirror M2. Another achromatic doublet L3 focuses the excitation beam on the back focal plane of the objective, which is mounted on a commercial inverted microscope Nikon ECLIPSE TE300. The 60X oil immersion objective (Nikon Plan Apo TIRF, 1.45 oil) produces a collimated excitation beam, for wide-field illumination, and collects the fluorescence signal emitted from the sample. The sample is mounted on a x, y piezo stage (P-527.2CL Phyisk Instrumente), while the objective can be moved along its optical axis through a piezo translator (P-721.C PIFOC Phyisk Instrumente). The dichroic mirror DM2 separates excitation from emission light, which passes through the emission filter FF prior to entering the detection path. For fluorescent beads imaging, Semrock LPD01-532RS-25 dichroic mirror and Semrock FF01-585/40 emission filter were used, whereas for Quantum Dot imaging (655 nm emission wavelength) Semrock FF500/646-Di01-25x36 dichroic mirror and Semrock FF01-655/40 emission filter were used. The microscope image is then projected by the tube lens L4 onto the EMCCD camera (Andor, Ixon X3), after an additional 3x magnification by the telescope L5, L6.

Pattern-Recognition Out-Of-Focus (PROOF) Imaging Software



Supplementary figure S 2 PROOF software interface.

PROOF is a custom-written software developed in Matlab for 3D localization of single fluorescent nanoparticles. PROOF automatically recognizes the number of rings in the diffraction pattern of single emitters and, according to this number, it selects an appropriate function to fit experimental data through weighted least squares method. PROOF opens, visualizes and analyzes images of diffraction patterns of both in-focus and out-of-focus fluorescent probes. PROOF allows selecting a Region Of Interest (ROI) that includes the image of the fluorescent particle and produces an output '.txt' file containing its x, y position as well as the radius of the outermost ring R_N (if any) of its diffraction pattern. By converting R_N to z through an appropriate calibration function, the axial position of the particle can be precisely determined.

The software is provided in the "PROOF" folder, which contains the main program (PROOF) and all the functions that are called from there. The "PROOF" folder should be added by the user through the File<Set path option in the Matlab window.

When PROOF is launched from the Matlab command window, the user is asked to browse for the file to be opened for analysis. PROOF can open stacks of '.tiff' images as well as single '.tiff' images. Once the image stack is completely uploaded, panels A and B, shown in figure S2, appear. Panel A is the Image Viewer, in which the image can be zoomed in and out, saved and displayed using the standard commands of Matlab windows.

Panel B is the Control Panel, through which additional visualization parameters as well as all the analysis parameters can be set.

By changing the position of the sliders highlighted by square 1 on the Control Panel, intensity level of the image can be adjusted to the desired values, to achieve optimal visualization for the user. The slider inside square 2 is used to browse through different

frames of the stack. Values in square 3 can be changed to select the range of frames to be analyzed.

“Displacement between frames” in square 4 represents the maximum distance (in nm) travelled by the particle per frame. The default value is zero, which is useful when the probe is not moving in the x-y plane, as during calibration. On the opposite, when this is set to a value different from 0, the ROI on which the analysis is performed (white square in panel A) is correspondingly enlarged between successive frames to find the new pattern center. In particular, the new center of the diffraction pattern is localized as either the maximum intensity pixel or as the ROI centroid, depending on the button “allow central hole” described below, and the ROI is centered on the new pattern center and resized to its original dimensions to analyze the frame.

The value “pause between frames” in square 4 allows the user to introduce a pause between the analysis of subsequent frames. This can be useful for visually inspecting images and fits during the analysis.

Additional options are available to users through the checkboxes highlighted by square 5. The “allow central hole” option should be selected for the analysis of Quantum Dot diffraction patterns in axial regions where they are transitioning between different numbers of rings. As described in the article, a peculiar feature of QDs is the appearance of a central hole in the diffraction intensity pattern at some axial positions. In these particular cases, the software will detect an even number of peaks, which is usually forbidden unless this button is pressed. If this option is enabled, whenever an even number of peaks is found, the user is asked to confirm this number, or to reject it by taking the number of peaks from the previous frame, or to skip the frame.

The “display on” option should be checked if the user wants to visualize the radial profile image (panel C) and the three-dimensional fit (panel D) during the analysis.

The “manual PSF center” option gives the opportunity to manually select the ROI center at each frame, by clicking on the desired position in the image viewer with the central mouse button. This option can be useful in cases in which automatic centering is not accurate (usually because of poor signal-to-noise ratio), which can especially deteriorate radial profile calculation.

Finally, the “threshold” value in square 6 must be set during the analysis of diffraction patterns of single QDs. In this case, whenever the average intensity within the ROI falls below the threshold value, typically because of blinking events, the frame is skipped. On the other hand, in the case of fluorescent beads, which are not affected by blinking, this parameter should be set to 0 (default value).

Before starting the analysis, the button “1:select ROI” must be pressed to select a region of interest in the image viewer. A white square can be drawn around the particle of interest, by selecting in sequence the top-left corner (left mouse click), the bottom-right corner (right mouse click) and the center of the ROI (middle mouse click). The middle mouse click terminates ROI selection. The ROI is always resized as square, for proper radial profile calculation. The ROI can be re-adjusted by pressing the “1:select ROI” button again.

The button “2: PROOF” should be pressed to start the analysis after all the analysis parameters are properly set and the ROI has been selected. Even so, all checkboxes as

well as “threshold”, “distance between frames”, and “pause between frames” can be modified while the analysis is running. The analysis is sequentially performed over the frame range selected by the user (square 3) as described below.

First, for each frame, the selected ROI is re-centered either on the pixel displaying the maximum intensity or on the ROI centroid, depending whether “allow central hole” is respectively off or on. Then, the average radial profile of the pattern is calculated, by step rotations around the ROI center and subsequent averaging. The result of this computation is displayed in the Radial Profile window (panel C). From the radial profile, the local maxima (peaks), i.e. data samples that are larger than their two neighboring samples, are detected and displayed in the Radial Profile window (green lines in panel C) and on the diffraction pattern image (red dots in panel A). The number, the coordinates and the amplitudes of peaks are used to calculate the initial parameters for the fitting function f described in details in the article. The fit is shown in the PSF fit window (panel D), in which the fitting function (red surface) is superimposed to the data (green).

After the last frame is analyzed, the user is requested to save the analysis results (described below in “the output file” section) to a desired location within the image stack directory. At this point, the user can change the analysis parameters and the ROI and start a new analysis. If a new ROI is not selected, the previous one is used.

Buttons “Abort” and “Quit” respectively terminate the analysis and the program. When “Abort” is pressed the analysis stops and analysis results can be saved up to the last frame analyzed. When “Quit” is pressed the program is closed without saving analyzed data. Alternatively, the program can be interrupted whenever desired by typing “ctrl+c” in the Matlab command window.

The Configuration file

```

91.11 nm/pixel camera_calibration
50 MIN_PEAK_HEIGHT+bgmean
3 MIN_PEAK_DISTANCE
9 N_PEAKS
-in_focus
0.11 P2
-1_ring
0.22 P2
0.15 P4=P2*...
-2_rings
0.22 P2
0.5 P4=P2*...
0.2 P6=P2*...
-3_rings
0.22 P2
0.5 P4=P2*...
0.4 P6=P2*... |
0.1 P8=P2*...
-4_rings
0.23 P2
1.2 P4=P2*...
0.5 P6=P2*...
0.6 P8=P2*...
0.13 P10=P2*...

```

Supplementary figure S 3 Configuration file.

A “PROOFconfig.txt” file allows the user to set additional analysis parameters, which mainly depends on the imaging system and microscope magnification (figure S3). This file should be placed in the same directory of the “PROOF.m” file.

The first parameter is the pixel size of the image (in nm/pixel). “MIN_PEAK_HEIGHT+bgmean”, “MIN_PEAK_DISTANCE”, and “N_PEAKS” are arguments of the ‘findpeaks’ Matlab function used for peaks detection from the average radial profile. “MIN_PEAK_HEIGHT+bgmean” is the minimum intensity value over the background for a peak to be detected. The background level is calculated as the average intensity over a 5x5 pixels matrix in the ROI top-left corner. “MIN_PEAK_DISTANCE” is the minimum allowed distance (in pixels) between adjacent local maxima (peaks). “N_PEAKS” is the maximum number of peaks that can be detected. In the present version (v1.0), the software can analyze diffraction patterns containing up to 9 peaks, correspondent to 4 Gaussian rings plus a central Gaussian peak.

The parameters listed below represent the initial guess for P2, which is related to the standard deviation of the central Gaussian profile σ_0 , and the initial guesses for P4, P6, P8 and P10, which are respectively related to the standard deviations of the Gaussian rings $\sigma_1, \sigma_2, \sigma_3, \sigma_4$, as defined in equation (1):

$$f = B_0 + A_0 \cdot \exp\left(-\frac{(x-x_0)^2 + (y-y_0)^2}{2\sigma_0^2}\right) + \sum_{i=1}^N A_i \cdot \exp\left(-\frac{\left(\sqrt{(x-x_0)^2 + (y-y_0)^2} - R_i\right)^2}{2\sigma_i^2}\right) \quad (1)$$

In particular, $P2 = 1/2\sigma_0^2$, $P4 = 1/2\sigma_1^2$, $P6 = 1/2\sigma_2^2$, $P8 = 1/2\sigma_3^2$ and $P10 = 1/2\sigma_4^2$. These values depend on the microscope magnification, on the camera pixel size, as well as optical aberrations that affects the PSF. These parameters can be set independently for fit functions with different number of rings (Fig. S3). In the configuration file, P2 is expressed as an absolute value, whereas P4-P10 are expressed as relative values to P2. For example, if the values in the configuration file for 1-ring function are P2=0.22 and P4=0.15, we get $\sigma_0 = 1/\sqrt{2*P2} = 1.51$ pixel and $\sigma_1 = 1/\sqrt{2*P4} = 1/\sqrt{2*0.15*P2} = 3.89$ pixel. In our setup, standard deviations of Gaussian rings are usually larger than the standard deviation of the central Gaussian profile, so that P4-P10 are usually <1.

Since P2-P10 depends on the optical setup only, they should be set once for a given setup. A way to set initial guesses is to make a z-scan of a single emitter and roughly measure the width of the central Gaussian profile and rings from the emitter images to set P2-P10. After one round of PROOF analysis, better estimates of the initial guesses can be obtained from average values of P2-P10 reported in the output file (see next section).

The other initial parameters for the fitting function, such as B_0 , A_0 , A_i , and R_i are measured automatically from the radial intensity profile and do not need any setting.

The configuration file can be modified before each “PROOF” analysis cycle and should be saved (as .txt, ANSI extension) for the changes to be applied.

The Output file

x pxls	y pxls	B ₀	A ₀	P ₂	A ₁	P ₄	R ₁	A ₂	P ₆	R ₂	A ₃	P ₈	R ₃	A ₄	P ₁₀	R ₄	fval
109.401121	103.415049	221.175915	2861.812829	0.178286	754.387643	0.214198	5.822172	483.822031	0.182800	11.809905	415.110037	0.118405	19.889330	570.981227	0.028015	32.873310	62111.878344
109.402920	103.438349	221.182878	2822.141516	0.180621	717.878389	0.205413	5.588742	497.919270	0.189718	11.845436	420.899318	0.117189	19.886213	571.041172	0.028134	32.803978	61700.720780
109.418400	103.449303	221.078805	2741.921279	0.173711	723.747431	0.197219	5.131413	492.730714	0.185883	11.798445	419.879509	0.115028	19.881814	570.900298	0.028190	32.818812	61888.477874
109.424815	103.452917	220.104424	3070.739215	0.188934	774.499219	0.217749	5.890176	488.031714	0.190889	11.054958	418.054434	0.121922	20.181340	566.181041	0.028120	33.100588	61000.487198
109.412007	103.439970	210.764844	3008.868818	0.181771	780.388211	0.218804	5.731149	483.387880	0.182443	11.058412	407.828383	0.120212	20.173789	558.341362	0.027924	33.118984	61481.388918
109.412811	103.417446	220.780182	2842.404817	0.188890	750.327071	0.219309	5.738417	447.126188	0.180877	11.038113	408.374699	0.120302	20.178013	548.197918	0.027948	33.108700	60400.718448
109.417507	103.473270	221.188199	2841.138411	0.188284	751.727187	0.218143	5.750823	449.423027	0.181304	11.064880	407.422431	0.121992	20.183881	550.888844	0.028438	33.112800	60184.038801
109.443929	103.474989	220.444481	3004.116313	0.183178	780.128890	0.200744	5.728430	458.116181	0.181993	11.044813	407.117780	0.121882	20.178471	551.407887	0.028007	33.108700	60170.781871
109.442798	103.462138	221.150080	3095.131238	0.190494	711.932170	0.218221	5.729888	449.913398	0.181212	11.037999	398.788787	0.121090	20.174217	541.950122	0.028199	33.108149	61144.283480
109.421002	103.468158	221.184109	2931.821211	0.181888	781.478609	0.218309	5.719000	450.981819	0.184847	11.044813	405.889185	0.121889	20.180407	541.024798	0.027877	33.107188	61011.381450
109.416188	103.473904	219.497998	3070.794012	0.181240	776.994833	0.218317	5.720999	458.177383	0.180581	11.049549	409.831711	0.123485	20.183182	551.857388	0.027886	33.119715	62038.888821
109.448188	103.474207	220.773884	3044.197100	0.189710	774.851811	0.218883	5.718488	454.901514	0.180581	11.037842	403.174337	0.123404	20.180814	551.198421	0.028113	33.124796	61980.750095
109.438737	103.491270	221.101117	3012.728880	0.184988	780.831327	0.217313	5.718493	454.974217	0.180901	11.017138	408.743902	0.123013	20.183773	550.181200	0.027989	33.133987	62000.106117
109.439774	103.488908	219.082838	3131.128119	0.214847	800.480230	0.217993	5.749951	452.932138	0.181970	11.047800	418.183388	0.123204	20.188711	549.138071	0.027915	33.127722	62174.997311
109.448903	103.488900	221.197333	3142.141139	0.218418	810.149091	0.218184	5.781150	461.889415	0.181583	11.056819	420.888153	0.124275	20.194201	549.498011	0.027921	33.131990	62148.811281
109.477840	103.488811	221.148406	3173.499212	0.208714	841.648181	0.218142	5.819113	461.880748	0.181173	11.111111	411.119138	0.126206	20.190109	548.808211	0.027781	33.121091	62148.811281
109.448801	103.448898	220.197187	3446.120710	0.218111	810.202851	0.218998	5.791219	454.760477	0.181745	11.188158	428.777729	0.121848	20.191189	571.021021	0.027820	33.127187	62174.141001
109.473884	103.459929	221.170188	3177.091910	0.218442	810.810201	0.218783	5.808004	458.188781	0.180818	11.028018	428.888887	0.126018	20.177149	549.274748	0.027898	33.107188	62011.888101
109.451948	103.451921	221.144178	3199.099719	0.210712	851.020211	0.218388	480.188714	458.188781	0.181879	11.131211	428.888887	0.126018	20.182145	549.907888	0.027911	33.121184	62011.888101
109.451948	103.451921	220.123171	3197.099719	0.209718	851.020211	0.218388	480.188714	458.188781	0.181879	11.131211	428.888887	0.126018	20.182145	549.907888	0.027911	33.121184	62011.888101
109.488421	103.488411	221.188113	3191.128919	0.219499	851.020211	0.218388	5.097318	458.188780	0.181375	11.088881	428.117790	0.127018	20.188881	570.119208	0.027803	33.124811	62199.188811
109.459820	103.442311	220.071898	3198.107118	0.207080	850.810919	0.218998	5.898212	451.709812	0.181811	11.128301	423.691823	0.126789	20.198481	568.228311	0.028131	33.121188	61380.028981
109.488421	103.488411	221.188113	3191.128919	0.219499	851.020211	0.218388	5.097318	458.188780	0.181375	11.088881	428.117790	0.127018	20.188881	570.119208	0.027803	33.124811	62199.188811
109.481138	103.482317	221.081890	3149.131493	0.218411	787.892919	0.200111	5.874013	418.189317	0.180907	11.114319	397.039821	0.124882	21.004414	540.184181	0.028007	34.180847	61111.178443
109.458023	103.481818	221.174818	3086.809844	0.216144	810.807627	0.218388	5.888388	458.000781	0.181937	11.087900	408.458003	0.126118	21.004414	541.188019	0.027813	34.119700	61111.178443
109.441921	103.413403	221.089200	3792.030983	0.244548	818.484841	0.219930	5.877974	428.792048	0.184988	11.147977	411.042838	0.128111	21.037174	547.087710	0.027488	34.171183	79977.248017
109.457121	103.450112	220.908713	3044.128119	0.248068	801.198219	0.218394	5.888460	421.121121	0.182312	11.080730	408.111289	0.128122	21.054282	540.708882	0.027451	34.182289	80388.002881

Supplementary figure S 4 Example of output file.

When the analysis is completed, the user is asked to save the analysis results. The output file is a '.txt' file in which data are organized as shown in figure S4. Each row corresponds to a frame ordered according to the frame sequence. The output file always starts from frame 1. If the analysis was performed from frame n>1, rows 1 to n are filled with zeros. "x pxls", "y pxls" are the coordinates of the center of the diffraction pattern, expressed in pixels. B₀, A_i, P_i and R_i are the parameters resulting from the fitting of the function f to the data. "fval" is the chi-square. In the example shown in figure S3, one central peak and 4 rings were detected and analyzed. In cases in which a lower number of rings is detected, higher-order parameters are filled with zeros.

Neuroblastoma cells

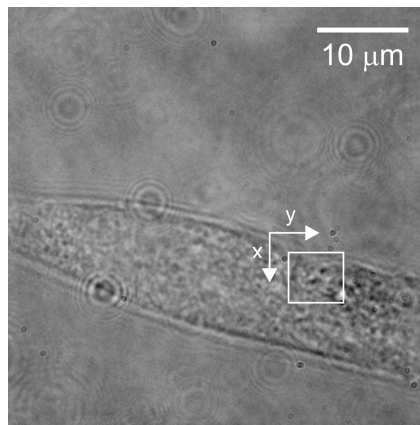


Figure S 5 Bright-field image of a neuroblastoma cell. White square and x-y axes correspond respectively to the region spanned by the QD trajectory and associated axes orientation in fig.4a.

Typical variations in calibration curves

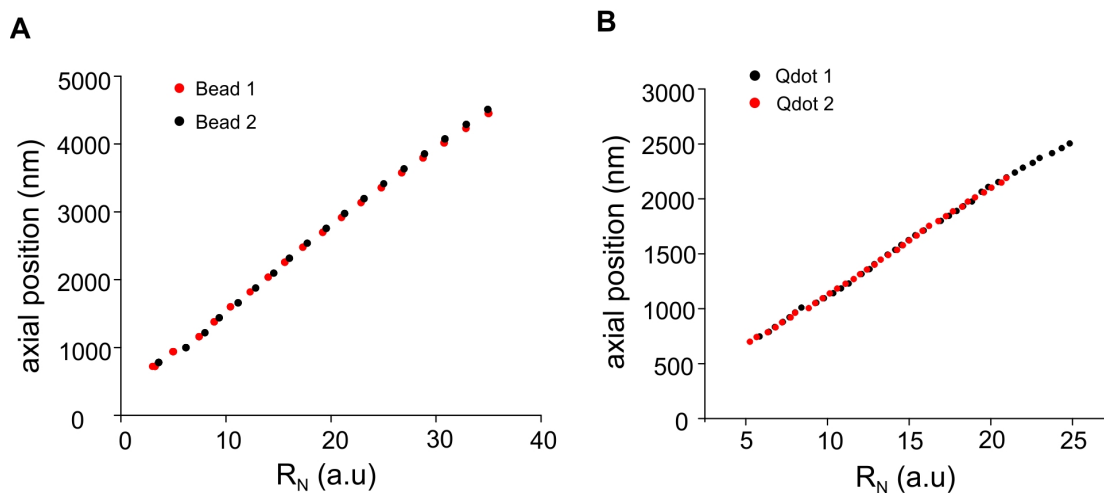


Figure S 6 A) Comparison between calibration curves obtained from two different fluorescent beads in 2% agarose. Bead 1 (red dots) is located on the coverslip surface, whereas Bead 2 (black dots) is located about 2.5 μm deep inside the gel. **B)** Comparison between calibration curves obtained from two different QDots attached on the cell membrane (saline buffer media) in independent experiments (red and black dots).

Lens aberrations can affect the PSF shape and thus introduce systematic errors in probe localization. Aberrations are strongly dependent on many different parameters such as the optical components (objective, tube lens, magnification optics), refractive index mismatches, and depth of the probe in the sample. Here we evaluate whether typical variations of probe distance from the coverslip surface or different experimental conditions might influence the axial calibration and thus localization accuracy.

Fig. S6a shows a comparison between two calibration measurements obtained in 2% agarose, from fluorescent beads located either at the glass coverslip surface (red dots) or 2.5 μm deep inside the gel (black dots). We sampled less points than in the calibration measurements displayed in Fig. 2 to avoid possible discrepancies between the two curves due to thermal drifts and fitted data points to get calibration curves as described in the article. We regarded variations in the distance between the two calibration curves as the error introduced by aberration effects owing to the different depth inside the sample. We quantified an average variation of 0.5 % in the axial region between 0.5 and 3.5 μm from the focal plane, and about 2 % between 3.5 and 4.5 μm .

Fig. S6b shows a comparison between calibration measurements obtained from two QDs attached to the membrane of two different neuroblastoma cells in two separate samples (black and red dots respectively). The two QDs were targeted to the membrane of fixed neuroblastoma cells as described in the article. Also in this case, we quantified variations in the distance between the two calibration curves, obtaining 0.5 % average variation over the entire calibration range.

Variation of axial localization accuracy with signal-to-background ratio

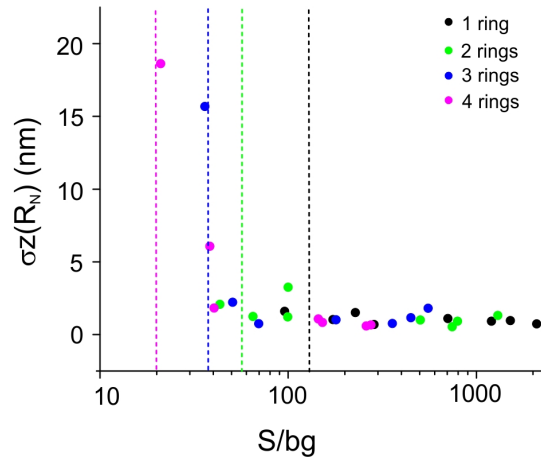


Figure S 7) Dependence of axial localization error $\sigma_z(R_N)$ on signal-to-background ratio (log scale) in the presence of different number of rings in the diffraction pattern. The number of rings is color coded according to the legend in the plot. Dashed lines in the plot represent the average value of S/bg measured during QD calibration (fig. 3 in the article) for different number of rings.

As shown in figure S7, we evaluated how fluorescence background impacts the localization accuracy. We measured the signal-to-background ratio (S/bg) of fluorescent nanobeads embedded in 2% agarose gel at four different axial positions, in which the PSF showed one to four diffraction rings. We varied the S/bg by changing the integration time and EMgain from 100 ms, 10X EMgain (same experimental conditions of the calibration described in the article) to 30 ms, no EMgain. S/bg ratio was calculated as

$$\frac{\langle I - bg \rangle}{\sigma_{bg}}$$

where I was calculated in a ROI surrounding the diffraction pattern and bg in an adjacent ROI of the same size, but containing no beads. $\langle I - bg \rangle$ as well as σ_{bg} (bg standard deviation) were calculated over 10 subsequent acquisitions under the same imaging conditions. Localization accuracy $\sigma_z(R_N)$ was calculated as the standard deviation of the localization over the 10 frames.

As shown in figure S7, the S/bg remains high and the localization accuracy stays within 2 nm when the diffraction pattern contains 1 or 2 rings, even at the fastest acquisition time. On the other hand, the S/bg diminishes when the number of rings increases to 3 and 4, thus affecting localization accuracy. Dashed lines in Fig. S7 represent the average value of S/bg measured during QD calibration (fig. 3 in the article) for different number of rings. It can be noticed that, for values of the S/bg correspondent to the far ends of QDs calibration curve, there is a rapid worsening of the axial localization accuracy up to a value of about 20 nm in the presence of 4 rings (about 2 μm from the focal plane), in accordance with what is shown in the article, Fig. 3c.

From these measurements, it emerges that fluorescence background level inside a live cell can influence localization accuracy especially at the farthest distances from the focal plane, and should thus be taken into account when evaluating localization accuracy.